https://doi.org/10.20965/ijat.2015.p0534

Paper:

Study on Nanoparticle Sizing Using Fluorescent Polarization Method with DNA Fluorescent Probe

Terutake Hayashi*, Yuki Ishizaki, Masaki Michihata**, Yasuhiro Takaya**, and Shin-ichi Tanaka*****

*Kyushu University
744 Motooka, Nishiku, Fukuoka, Fukuoka 819-0395, Japan
E-mail: thayashi@mech.kyushu-u.ac.jp
**Osaka University
2-1 Yamadaoka, Suita, Osaka 565-0871, Japan
***Kure National College of Technology
2-2-11 Agaminami, Kure, Hiroshima 737-8506, Japan
[Received March 24, 2015; accepted May 7, 2015]

Fluorescent polarization methods are used to detect complementary base pairing of DNA in biological fields. These methods work by measuring the rotational diffusion coefficient of Brownian motion of the fluorescent particles in solution. The rotational diffusion coefficient corresponds to the inverse third power of diameter according to the Debye-Stokes-Einstein equation for nanoparticles as hard spheres. We develop a novel method to measure the rotational diffusion coefficient using a fluorescent probe with a DNA spacer connected to a gold nanoparticle. We studied the physical characteristics of this probe to verify the feasibility of the proposed method. The rotational diffusion coefficients of gold nanoparticles with diameters ranging between 5–20 nm were measured using this developed system. In this manuscript we describe a novel fluorescent polarization method for nanoparticle sizing using a fluorescent DNA probe.

Keywords: nanoparticle sizing, fluorescent DNA probe, gold nanoparticle, fluorescent polarization, rotational diffusion coefficient

1. Introduction

Controlling the size of metal nanoparticles and monitoring their aggregational state are important considerations for manufacturing functional nanostructure devices [1–5]. We suggest a particle sizing method based on the analysis of rotational Brownian motion. The average size of particles can be estimated from the rotational diffusion coefficient, which represents the rotational speed of Brownian motion. The rotational diffusion coefficient of a particle can be measured by analyzing the polarization direction of fluorescence emitted from a fluorescent probe labeled on the particle.

When measuring the rotational diffusion coefficient of a rigid, spherical, and fluorescent particle, the rotational diffusion coefficient D_r can be described by the Debye-Stokes-Einstein equation [6–8]:

$$D_r = \frac{k_B T}{\pi d^3 \eta} \quad \cdots\cdots\cdots\cdots\cdots\cdots (1)$$

where k_B is the Boltzmann constant, T is the temperature, η is the viscosity of the solvent, and d is the particle diameter. Eq. (1) shows that the rotational diffusion coefficient is proportional to the inverse third power of the particle diameter.

In this study, we developed a system to measure the rotational diffusion coefficients of fluorescent particles and a fluorescent DNA (fl-DNA) probe that can be used to label particles. When excited, fluorescent probes emit a polarized fluorescence signal that can be analyzed to determine the size of the particles labeled with the probes.

Using this fluorescent polarization method, we investigated the physical characteristics of the fl-DNA probe connected to a metal nanoparticle and determined its rotational diffusion coefficient. The rotational diffusion coefficient of the unlabeled metal nanoparticle was also analyzed to verify the feasibility of particle sizing using fluorescent polarization [9–11].

2. Rotational Diffusion Coefficient Measurement Using DNA Probe

A standard coordinate system for evaluating fluorescence anisotropy is shown in **Fig. 1**. $I_{\parallel}$ and $I_{\perp}$ are components of fluorescence intensity that are parallel and perpendicular, respectively, to the direction of polarization of the excitation light. **Fig. 2** shows the variation over time in the rotational motion of the fluorophore and the polarization direction of the fluorescence emitted from the fluorescent probe in the *x-y* plane. The fluorophore has absorption and emission moments and is excited by light with polarization parallel to the absorption moment. The

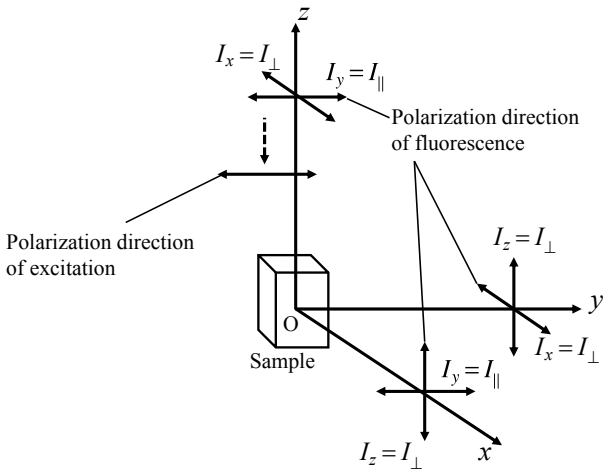

Fig. 1. Standard coordinate system.

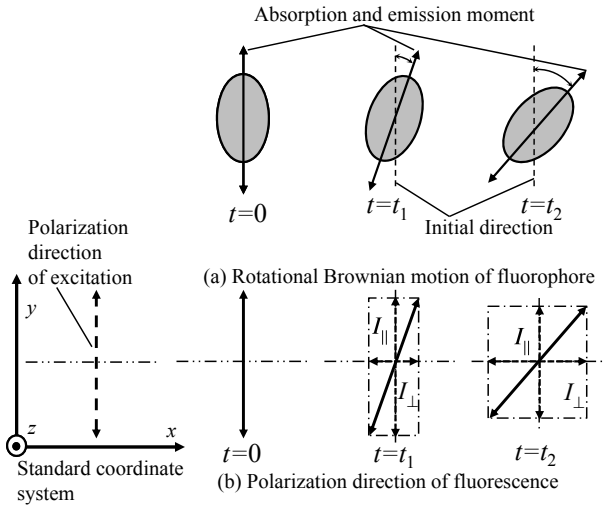

Fig. 2. Relationship between rotational Brownian motion and the polarization direction of fluorescence.

fluorescence anisotropy [9] can be described by

$$r(t) = \frac{I_\parallel(t) - I_\perp(t)}{I_\parallel(t) + 2I_\perp(t)}. \quad \ldots\ldots\ldots\ldots \quad (2)$$

Assuming that the sample is a spherical rigid rotor, $r(t)$ is described by

$$r(t) = r_0 \exp\left(-\frac{t}{6D_r}\right). \quad \ldots\ldots\ldots\ldots \quad (3)$$

3. Experimental Setup

3.1. Structure of the Fluorescent Probe

The experimental setup is shown in **Fig. 3**. A linearly polarized laser with 488 nm wavelength is the excitation light. The symbols L, M, and DM indicate the lens, mirror, and dichroic mirror, respectively. The amplitude of the excitation light is modulated into a sinusoidal wave-

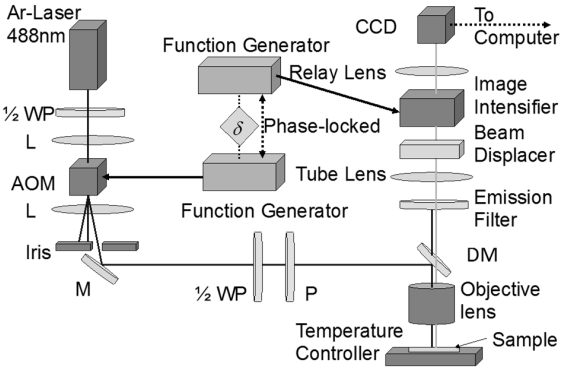

Fig. 3. Experimental setup.

form when passed through an acousto-optic modulator (AOM). After the polarization direction of the excitation light is adjusted to be along the y-axis by a half-wave plate (1/2 WP) and polarizer (P), the excitation light is focused onto the sample through the objective lens.

The excitation beam, which is defined in **Fig. 1**, corresponds to the light traveling from the objective lens to the sample as shown in **Fig. 3**. We define the propagation direction of the excitation light as the z-axis in the coordinate system as shown in **Fig. 1**. The x- and y-axes could be rotated in **Fig. 3** and defined based on the polarization direction of the excitation light. The x-axis is perpendicular to the polarization direction of the excitation light, and the y-axis is parallel to the polarization direction of the excitation light.

The fluorescence emitted from the sample passes along the z-axis through the dichroic mirror and emission filter, while the reflected excitation light from the sample is blocked by these two components. The beam displacer divides the fluorescence into two orthogonal oriented polarization signals, $I_\parallel$ and $I_\perp$.

Both $I_\parallel$ and $I_\perp$ are evaluated by analyzing the brightness of the fluorescent spot in the image captured by the CCD camera. A sinusoidally modulated fluorescence signal is obtained by shifting the phase of the trigger signal of the image intensifier. The period of the trigger signal is synchronized with the period of the modulation signal of the AOM. When the phase of the enhanced fluorescence signal is shifted, we scan the phase shift for as much as two cycles from 0° to 720°.

Figure 4 shows the relationship between the intensity of the excitation light and that of the emitted fluorescent light. The solid line shows the excitation light intensity and the short dashed line shows the emitted fluorescent light intensity. The fluorescent signal can be resolved into two components based on the direction of polarization. The signal with polarization parallel to the excitation light is shown as a double-dotted chain line. The average intensity is $I_{0\parallel}$, and the amplitude of the intensity modulation is $A_\parallel$. The phase of the modulation is $\phi_\parallel$. The signal with polarization perpendicular to the excitation light is shown as a chain line. The average intensity is $I_{0\perp}$, the amplitude of the intensity modulation $A_\perp$, and the phase of the mod-

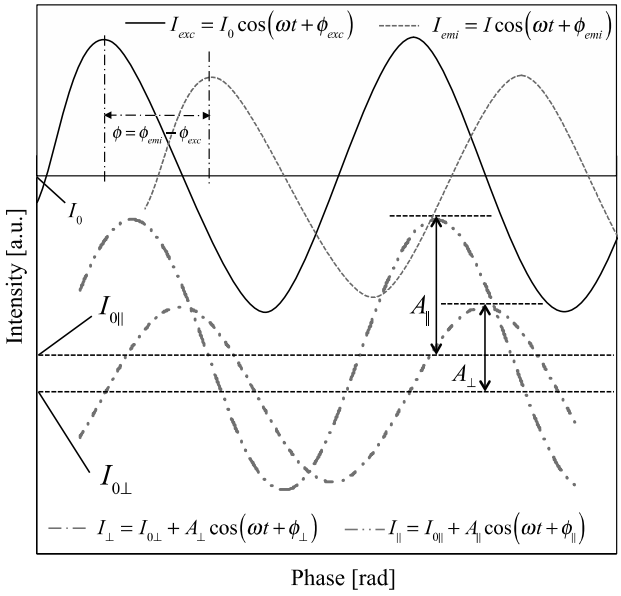

Fig. 4. Schematic of modulated fluorescent light.

ulation $\phi_\perp$. Based on the analysis of fluorescent signals, we can obtain the rotational correlation time parameters Y_{DC} and Y_{AC} from the amplitude and intensity of polarized fluorescence emission as shown in Eqs. (4) and (5). We can calculate the rotational diffusion coefficient D_r based on Y_{DC} and Y_{AC} as previously described for fluorescence anisotropy imaging by microscopy [10].

$$Y_{DC} = \frac{I_{0\parallel}}{I_{0\perp}} \quad \ldots\ldots\ldots\ldots\ldots\ldots \quad (4)$$

$$Y_{AC} = \frac{A_\parallel}{A_\perp} \quad \ldots\ldots\ldots\ldots\ldots\ldots \quad (5)$$

3.2. Conjugation of fl-DNA Probe with Nanoparticles

We arranged the fl-DNA probe on nanoparticles by forming thiol self-assembled monolayers (SAMS). Thiol SAMs are important in the synthesis of gold nanoparticles to stabilize the nanostructures against aggregation and to control the cluster size by tuning the hydrocarbon chain length. We consider that the fl-DNA construct works both as a probe to detect the rotational diffusion coefficient and as a coating to keep the size of gold nanoparticles static during the particle sizing procedure [12].

The fl-DNA probe is comprised of three parts: (1) a sulfur headgroup, which forms a strong, covalent bond with the particle surface, (2) a double-stranded DNA spacer, which stabilizes the SAM through van der Waals interactions, and (3) a fluorophore, which emits a fluorescence signal upon excitation. The 3'-thiol modified DNA can be adsorbed onto gold surfaces (Au[111]), in which intermolecular forces play a key role. It can also attach to other metallic surfaces including those composed of Ag, Cu, Pd, Pt, Ni, and Fe, and semiconductor surfaces such as GaAs and InP [12].

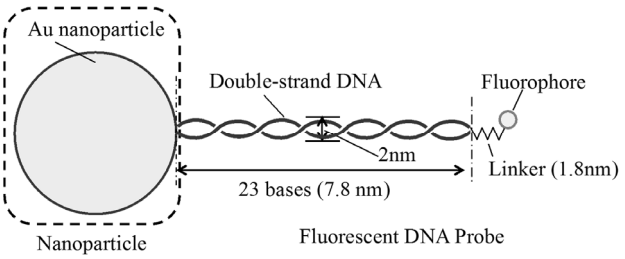

Fig. 5. Schematic of the fluorescent DNA probe.

In general, adsorption is performed in 10–1000 μM solutions of thiols. Initially a physisorption step occurs, followed by chemisorption of the molecules.

After physisorption, thiol molecules chemisorb onto the Au(111) substrate through the S headgroup, forming a strong covalent bond in a process that takes at least a few minutes. During this process, the thiol molecule loses the mercaptan H atom and is transformed into a thiolate. We can write the adsorption process as follows

$$\mathrm{R_nSH + Au \rightarrow (R_nSH)_{phys}Au} \quad \ldots\ldots\ldots \quad (6)$$

$$\mathrm{R_nSH_{phys}Au \rightarrow R_nS - Au + \frac{1}{2}H_2} \quad \ldots\ldots\ldots \quad (7)$$

where R is the 3' end of the DNA spacer and the reactions in Eqs. (6) and (7) correspond to thiol physisorption and chemisorption, respectively.

4. Fundamental Properties of the DNA Probe

4.1. Structure of the Fluorescent Probe

In order to measure the rotational diffusion coefficient of the nanoparticles, we need the fl-DNA probe to label the particles. However, fluorophores directly attached to a metal nanoparticle are quenched because of surface energy transfer (SET) from the fluorophore to the metal nanoparticle. The energy transfer efficiency is described by Eq. (8) [13].

$$\Phi_{EnT} = \frac{1}{1 + \left(\frac{l}{l_0}\right)^4} \quad \ldots\ldots\ldots\ldots\ldots \quad (8)$$

where l is the distance between the fluorophore and nanoparticle and l_0 is called the Forster distance, which is the distance at which the energy transfer efficiency is 50%.

We can control the length of the DNA spacer component of the fl-DNA probe by varying the number of base pairs in the DNA molecule. Through reaction of the metal nanoparticle with 3'-thiol and 5'-fluorophore modified DNA [14], the probe attaches to the surface of the metal particle, as shown in **Fig. 5**. We used DNA containing 23 base pairs as a spacer. Given the lengths of the particle-thiol and DNA-fluorophore linkers (∼1.8 nm)

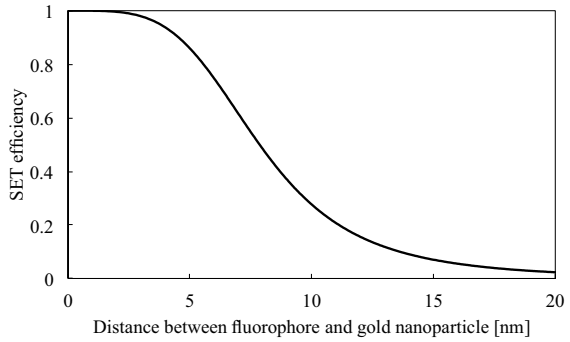

Fig. 6. Quenching of fl-DNA due to SET.

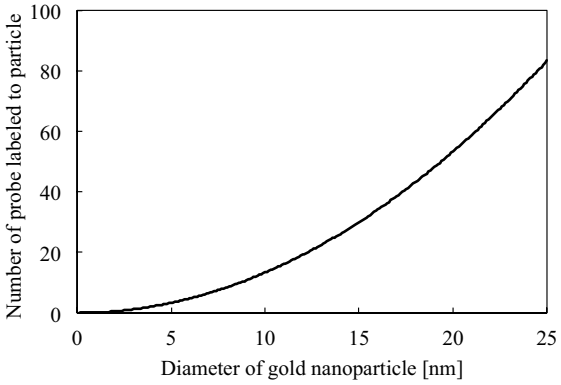

Fig. 7. Number of fl-DNA molecules on the gold nanoparticles.

the distance between the fluorophore and metal particle is about 9.6 nm, which is longer than the Forster distance, 9 nm, calculated in the case of energy transfer from an organic fluorophore to a gold nanoparticle [13].

Figure 6 shows the SET efficiency against the distance l_0 between the fluorophore and nanoparticle based on Eq. (9) [15].

$$l_0 = \left(\frac{0.225 c^3 \Phi_{dye}}{\omega_{dye}^2 \omega_F k_F} \right)^{\frac{1}{4}} \quad \ldots\ldots\ldots\ldots \quad (9)$$

where c is the speed of light, Φ_{dye} is the quantum efficiency of the fluorophore and ω_{dye} is its frequency of electron transition, ω_F is the Fermi frequency, and k_F is the wave number vector of the metal nanoparticle. Therefore, the energy transfer efficiency is below 50%, and sufficient fluorescence intensity can be obtained to perform measurements.

Based on the energy transfer calculation, DNA containing 23 base pairs should block at least 50% of SET to the gold nanoparticle. We consider the fl-DNA probe with 23 DNA base pairs to be bright enough as a fluorescent probe to evaluate the rotational diffusion coefficient. In addition, we consider that the short spacer has the advantage that gold nanoparticles with bound fl-DNA probes approximate the simple rotational motion of a smooth sphere.

4.2. Number of fl-DNA Probes on Nanoparticles

The number of fl-DNA probes attached to the surfaces of nanoparticles can be determined experimentally. Hurst et al. investigated the coverage of DNA molecules on gold nanoparticles [16]. They measured the number of DNA molecules attached to gold nanoparticles with diameters varying from 15–250 nm. The results show that the maximum density of DNA molecules on gold nanoparticles is constant among nanoparticles of different diameters. The maximum density of DNA molecules containing 10 base pairs is described as 4.24×10^{10} /cm^2 for the surfaces of gold nanoparticles.

Based on these results, we estimated the number of DNA molecules on gold nanoparticles with diameters of 0–25 nm with the assumption that the surface DNA loading density is fixed as 4.24×10^{10} /cm^2. **Fig. 7** shows DNA loading as a function of nanoparticle size. As shown in **Fig. 7**, the maximum number of DNA molecules on particles of 8.2 nm in diameter is about 10. In the case of 20 nm particles, we estimate that the number of attached fl-DNA molecules is smaller than 60. We consider that the number of attached fl-DNA molecules is less enough to precisely evaluate the rotational diffusion coefficients of the nanoparticles.

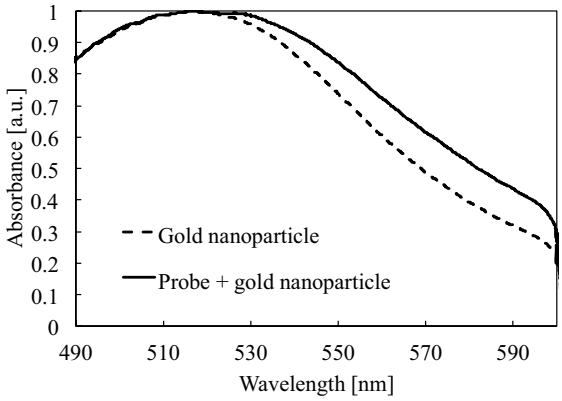

Fig. 8. Absorbance spectra of gold nanoparticles.

5. Absorbance Peak Shift of Labeled Nanoparticles

The absorbance peak of gold nanoparticles is known to be shifted to a longer wavelength range when they are coated with dielectrics such as DNA [17]. We used this phenomenon to check the attachment of fl-DNA probes onto the gold nanoparticles. We prepared bare gold nanoparticles (8.2 nm in mean diameter) and gold nanoparticles with fl-DNA probe. The absorbance peak of bare gold nanoparticles was near 520 nm.

Figure 8 shows a comparison of the absorbance spectra of the bare and DNA functionalized gold nanoparticles. The absorbance spectrum of gold nanoparticles with fl-DNA was shifted to a longer wavelength compared with that of bare gold nanoparticles. The peak shift

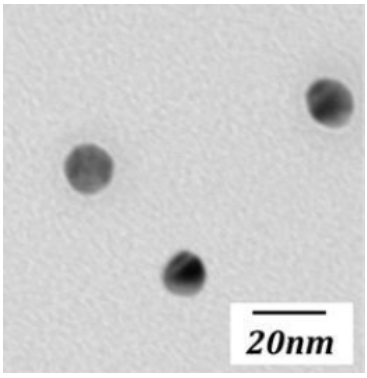

Fig. 9. TEM image of gold nanoparticles with a nominal mean diameter of 8.2 nm.

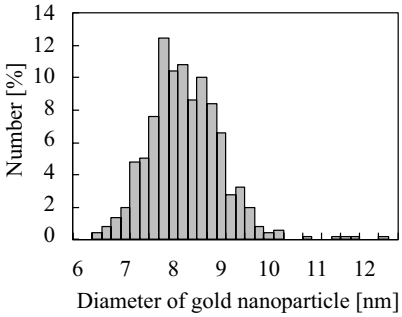

Fig. 10. Histogram of particle diameter distribution for particles with a nominal mean diameter of 8.2 nm, measured by TEM. The distribution can be approximated as Gaussian.

corresponded with the shift expected when dielectrics are coated onto the gold nanoparticle. From the above results, we can confirm the labeling of fl-DNA probe onto the nanoparticle surface.

6. Comparison of Rotational Diffusion Coefficients

We measured the rotational diffusion coefficients of gold nanoparticles with a nominal mean diameter of 8.2 nm. **Fig. 9** shows a transmission electron microscopy (TEM) image, which revealed that the particles are spherical in shape. **Fig. 10** shows the typical distribution of the diameters of gold nanoparticles.

Figure 11 shows the particle diameter distribution as determined by a dynamic light scattering method. As shown in **Figs. 10** and **11**, the distribution of particle diameters is narrow (5–15 nm), and the measured mean diameter is near 8 nm.

We prepared two samples. One is the fl-DNA probe containing a DNA spacer of 23 base pairs. The other is the bare gold nanoparticle labeled with fl-DNA. The rotational diffusion coefficients were evaluated by varying the temperature of the solvent using the measurement system shown in **Fig. 3**.

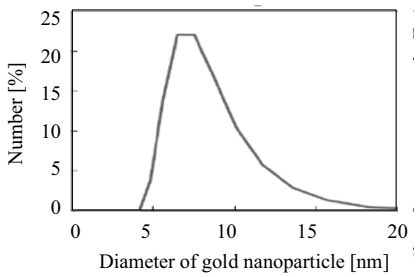

Fig. 11. Particle diameter distribution for particles with a nominal mean diameter of 8.2 nm measured by dynamic light scattering.

Table 1. Relationship between temperature and viscosity.

Temperature T [K]	Viscosity η [mPa s]	T/η [K/mPa s]
293	1.002	292.4
298	0.890	334.8
303	0.797	380.2
308	0.719	428.4
313	0.653	479.3

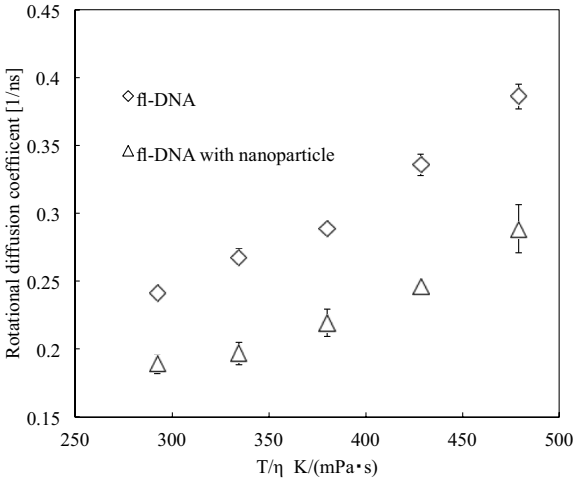

Fig. 12. Rotational diffusion coefficient by varying T/η.

The temperature of the solvents was maintained at 293 K, 298 K, 303 K, 308 K, 313 K, the modulation frequency was set to 60 MHz, and the values were averaged from 10 experimental trials. When we alter the temperature, the viscosity is also changed. **Table 1** shows the relationships among T, η, and T/η. The rotational diffusion coefficients of the fluorescent DNA probes connected to gold nanoparticles are shown in **Fig. 12**. The horizontal axis shows T/η, which indicates particle mobility in the solvent. The vertical axis shows the rotational diffusion coefficient and error bars show the standard deviation of measurements. The plot is sequentially aligned from left at 293 K, 298 K, 303 K, 308 K, and 313 K, respectively.

The rotational diffusion coefficient is sensitive to the

mobility of nanoparticles in this condition as shown in **Fig. 12**. It is considered that the gap in the values of the rotational diffusion coefficient between fl-DNA alone and fl-DNA attached to the gold nanoparticle can provide information about the sizes of the gold nanoparticles.

D_r linearly increased with T/η for both the fl-DNA probe and the fl-DNA probe connected to gold nanoparticles. These findings matched the predictions of Eq. (1) well.

However, nonlinearity appeared in the range over 313 K. We have to investigate the reasons for the nonlinear change in the range over 313 K. We have two hypotheses; one is simply a decrease in the viscosity of the solvent, and the other is the disaggregation of DNA in the higher temperature range.

From the above results, we confirm the feasibility of evaluating the rotational diffusion coefficient of nanoparticles whose size is smaller than 10 nm in the range 293–313 K based on the linear relationship between D_r and T/η.

The rotational diffusion coefficient measured using the proposed method is not that of the gold nanoparticle itself, but rather is that of the fl-DNA probe connected with the gold nanoparticles. Thus, we need to confirm the relationship between the rotational diffusion coefficient of gold nanoparticles and that of fl-DNA probes connected to the particles.

7. Conclusion

In order to verify the feasibility of the proposed nanoparticle sizing method, fundamental experiments were performed. The rotational diffusion coefficient of the fluorescent DNA probe (fl-DNA) was measured precisely using the developed system.

We measured the rotational diffusion coefficients of gold nanoparticles with a nominal mean diameter of 8.2 nm. The rotational diffusion coefficients decrease with the mobility of fl-DNA. The results indicate that nanoparticles with diameters smaller than 15 nm can be sized using the proposed method.

Acknowledgements

This research was partly supported by Japan Society for the Promotion of Science (JSPS) Grants-in-Aid for Scientific Research (Number 24656088).

References:

[1] R. G. Freeman et al., "Self-assembled metal colloid monolayers: An approach to SERS substrates," Science, Vol.267, No.5204, pp. 1629-1632, 1995.
[2] S. Sun et al., "Monodisperse FePt nanoparticles and ferromagnetic FePt nanocrystal superlattices," Science, Vol.287, No.5460, pp. 1989-1992, 2000.
[3] D. L. Feldheim et al., "Electron transfer in self-assembled inorganic polyelectrolyte/metal nanoparticle heterostructures," J. Am. Chem. Soc., Vol.118, No.32, pp. 7640-7641, 1996.
[4] R. P. Andres et al., "Self-assembly of a two-dimensional superlattice of molecularly linked metal clusters," Science, Vol.273, pp. 1690-1693, 1987.
[5] A. N. Shipway et al., "Nanoparticle arrays on surfaces for electronic, optical, and sensor applications," Chem. Phys. Chem., Vol.1, pp. 18-52, 2000.
[6] P. Debye, "Polar Molecules," Dover, 1929.
[7] P. P. Jose et al., "Complete breakdown of the Debye model of rotational relaxation near the isotropic-nematic phase boundary: Effects of intermolecular correlations in orientational dynamics," Phys. Rev. E, Vol.73, No.3, p. 031705, 2006.
[8] L. Andreozzi et al., "Evidence of a fractional Debye-Stokes-Einstein law in supercooled o-terphenyl," Europhys. Lett., Vol.38, No.9, pp. 669-674, 1997.
[9] K. Kinosita et al., "A theory of fluorescence polarization decay in membranes," Biophys. J., Vol.20, No.3, pp. 289-305, 1977.
[10] A. H. A. Clayton et al., "Dynamic fluorescence anisotropy imaging microscopy in the frequency domain (rFLIM)," Biophys. J., Vol.83, No.3, pp. 1631-1649, 2002.
[11] R. D. Spencer and G. Weber, "Measurements of subnanosecond fluorescence lifetimes with a cross-correlation phase fluorometer," Annals of the New York Academy of Science, Vol.158, No.1, pp. 361-376, 1969.
[12] C. Vericat, et al., "Self-assembled monolayers of thiols and dithiols on gold: new challenges for a well-known system," Chem. Soc. Rev., Vol.39, No.5, pp. 1805-1834, 2010.
[13] C. S. Yun et al., "Nanometal surface energy transfer in optical rulers breaking the FRET barrier," J. Am. Chem. Soc., Vol.127, No.9, pp. 3115-3119, 2005.
[14] H. Morimura et al., "Nano-analysis of DNA conformation changes induced by transcription factor complex binding using plasmonic nanodimers," ACS Nano., Vol.12, pp. 10733-10740, 2013.
[15] T. Sen et al., "Surface energy transfer from rhodamine 6G to gold nanoparticles A spectroscopic ruler," Applied physics letters, Vol.91, p. 1033, 2007.
[16] S. J. Hurst et. al., "Maximizing DNA loading on a range of gold nanoparticle sizes.," Anal. Chem., Vol.78, No.24, pp. 8313-8318, 2006.
[17] M. N. Bui et al., "Gold nanoparticle aggregation-based highly sensitive DNA detection using atomic force microscopy," Anal. Bioanal. Chem, Vol.388, pp. 1185-1190, 2007.

Name:
Terutake Hayashi

Affiliation:
Department of Mechanical Engineering, Graduate School of Engineering, Kyushu University

Address:
744 Motooka, Nishi-ku, Fukuoka-shi, Fukuoka 565-0395, Japan

Brief Biographical History:
2001- Research Associate, Research Center for Superplasticity, Ibaraki University
2005- Research Associate, Osaka University
2010- Associate Professor, Osaka University
2014- Associate Professor, Kyushu University

Main Works:
• T. Hayashi, Y. Ishizaki, M. Michihata, Y. Takaya, and S. Tanaka, "Nanoparticle sizing method based on fluorescence anisotropy analysis," Measurement, Vol.59, pp. 382-388, 2015.

Membership in Academic Societies:
• Japan Society for Precision Engineering (JSPE)
• Japan Society of Mechanical Engineers (JSME)

Name:
Yuki Ishizaki

Affiliation:
Staff, Memory Design Engineer, Toshiba Corporation Semiconductor & Storage Products Company

Address:
3-2-7 Namiki, Kanazawa-ku, Yokohama-shi, Kanagawa 236-0005, Japan

Brief Biographical History:
2014- Toshiba Corporation Semiconductor & Storage Products Company

Main Works:
• "Study on Measurement of Nanoparticles Size Based on Fluorescence Polarization (1st Report) – Development of Rotational Diffusion Coefficient Measurement System Using Fluorescent DNA Probe," J. of the Japan Society for Precision Engineering, Vol.80, No.2, pp. 214-219, 2014.

Name:
Masaki Michihata

Affiliation:
Assistant Professor, Research Center of Advanced Science and Technology, The University of Tokyo

Address:
4-6-1 Komaba, Meguro, Tokyo 153-8904, Japan

Brief Biographical History:
2010- Assistant Professor, Osaka University
2015- Assistant Professor, The University of Tokyo

Main Works:
• "Measurement of probe-stylus sphere diameter for micro-CMM based on spectral fingerprint of whispering gallery modes," CIRP Annals-Manufacturing Technology, Vol.63, No.1, pp. 469-472, 2014.

Membership in Academic Societies:
• Japan Society for Precision Engineering (JSPE)
• Japan Society of Mechanical Engineers (JSME)

Name:
Yasuhiro Takaya

Affiliation:
Department of Mechanical Engineering, Graduate School of Engineering, Osaka University

Address:
2-1 Yamadaoka, Suita, Osaka 565-0871, Japan

Brief Biographical History:
1992 Received Ph.D. degree (Engineering)
1992- Research Associate, Osaka University
1995- Assistant Professor, Osaka University
1997- Associate Professor, Osaka University
2006- Professor, Osaka University

Main Works:
• Y. Takaya, M. Michihata, T. Hayashi, and T. Washitani, "Dimensional measurement of microform with high aspect ratio using an optically controlled particle with standing wave scale sensing," Annals of the CIRP, Vol.61, Issue 1, pp. 479-482, 2012.
• Y. Takaya, M. Michihata, T. Hayashi, R. Murai, and K. Kano, "Surface analysis of the chemical polishing process using a fullerenol slurry by Raman spectroscopy under surface plasmon excitation," Annals of the CIRP, Vol.62, Issue 1, pp. 571-574, 2013.

Membership in Academic Societies:
• Japan Society for Die and Mould Technology (JSDMT), Vice President
• Japan Society of Precision Engineering (JSPE)
• Japan Society of Mechanical Engineers (JSME)
• American Society for Precision Engineering (ASPE)
• Japan Society for Abrasive Technology (JSAT)
• International Academy of Production Engineering (CIRP), Fellow

Name:
Shin-ichi Tanaka

Affiliation:
Kure National College of Technology

Address:
2-2-11 Agaminami, Kure, Hiroshima 737-8506, Japan

Brief Biographical History:
2004- Research Fellowships for Young Scientists, Japan Society for the Promotion of Science (JSPS)
2007- Postdoctoral Fellow, RIKEN
2007- Postdoctoral Fellow, Graduate School of Frontier Biosciences, Osaka University
2009- Special-Appointment Assistant Professor, Graduate School of Frontier Biosciences, Osaka University
2011- Postdoctoral Fellow, Graduate School of Engineering, Osaka University
2012- Associate Professor, Kure National College of Technology

Main Works:
• "Synthesis of Fluorescent Platinum Nanoclusters for Biomedical Imaging," Functional Nanometer-Sized Clusters of Transition Metals: Synthesis, Properties and Applications, The Royal Society of Chemistry, Chapter 13, pp. 391-406, 2014.

Membership in Academic Societies:
• American Chemical Society (ACS)
• Chemical Society of Japan (CSJ)
• Biophysical Society of Japan (BSJ)